

University of Groningen

Chromogranin A regulates gut permeability via the antagonistic actions of its proteolytic peptides

Muntjewerff, Elke M; Tang, Kechun; Lutter, Lisanne; Christoffersson, Gustaf; Nicolassen, Mara J T; Gao, Hong; Katkar, Gajanan D; Das, Soumita; Ter Beest, Martin; Ying, Wei

Published in:
Acta physiologica

DOI:
[10.1111/apha.13655](https://doi.org/10.1111/apha.13655)

IMPORTANT NOTE: You are advised to consult the publisher's version (publisher's PDF) if you wish to cite from it. Please check the document version below.

Document Version
Publisher's PDF, also known as Version of record

Publication date:
2021

[Link to publication in University of Groningen/UMCG research database](#)

Citation for published version (APA):

Muntjewerff, E. M., Tang, K., Lutter, L., Christoffersson, G., Nicolassen, M. J. T., Gao, H., Katkar, G. D., Das, S., Ter Beest, M., Ying, W., Ghosh, P., Aidy, S. E., Oldenburg, B., van den Bogaart, G., & Mahata, S. K. (2021). Chromogranin A regulates gut permeability via the antagonistic actions of its proteolytic peptides. *Acta physiologica*, 232(2), [e13655]. <https://doi.org/10.1111/apha.13655>

Copyright

Other than for strictly personal use, it is not permitted to download or to forward/distribute the text or part of it without the consent of the author(s) and/or copyright holder(s), unless the work is under an open content license (like Creative Commons).


The publication may also be distributed here under the terms of Article 25fa of the Dutch Copyright Act, indicated by the "Taverne" license. More information can be found on the University of Groningen website: <https://www.rug.nl/library/open-access/self-archiving-pure/taverne-amendment>.

Take-down policy

If you believe that this document breaches copyright please contact us providing details, and we will remove access to the work immediately and investigate your claim.

Downloaded from the University of Groningen/UMCG research database (Pure): <http://www.rug.nl/research/portal>. For technical reasons the number of authors shown on this cover page is limited to 10 maximum.

Chromogranin A regulates gut permeability *via* the antagonistic actions of its proteolytic peptides

Elke M. Muntjewerff¹ | Kechun Tang² | Lianne Lutter^{3,4} | Gustaf Christoffersson^{5,6} |
Mara J. T. Nicolassen¹ | Hong Gao⁷ | Gajanan D. Katkar⁸ | Soumita Das⁹ |
Martin ter Beest¹ | Wei Ying⁷ | Pradipta Ghosh^{7,8} | Sahar El Aidy¹⁰ | Bas Oldenburg⁴ |
Geert van den Bogaart^{1,10} | Sushil K. Mahata^{2,7} 

¹Department of Tumor Immunology, Radboud Institute for Molecular Life Sciences, Radboud University Medical Center, Nijmegen, the Netherlands

²VA San Diego Healthcare System, San Diego, CA, USA

³Center for Translational Immunology, Utrecht University Medical Center, Utrecht, the Netherlands

⁴Department of Gastroenterology and Hepatology, Utrecht University Medical Center, Utrecht, the Netherlands

⁵Science for Life Laboratory, Uppsala University, Uppsala, Sweden

⁶Department of Medical Cell biology, Uppsala University, Uppsala, Sweden

⁷Department of Medicine, University of California San Diego, La Jolla, CA, USA

⁸Department of Cellular and Molecular Medicine, University of California San Diego, La Jolla, CA, USA

⁹Department of Pathology, University of California San Diego, La Jolla, CA, USA

¹⁰Department of Molecular Immunology and Microbiology, Groningen Biomolecular Sciences and Biotechnology Institute, University of Groningen, Groningen, the Netherlands

Correspondence

Geert van den Bogaart, Department of Molecular Immunology, University of Groningen, the Netherlands.
Email: g.van.den.bogaart@rug.nl

Sushil K. Mahata, VA San Diego Healthcare System, San Diego, CA, USA.
Email: smahata@health.ucsd.edu

Funding information

Veterans Affairs San Diego Healthcare System, Grant/Award Number: I01 BX003934; European Research Council, Grant/Award Number: 862137; Human Frontier Science Program, Grant/Award Number: RGY0080/2018; Netherlands Organization for Scientific Research, Grant/Award Number: NWO-ALWVIDI864.14.001; Swedish Research Council; Swedish Society for Medical Research; Rosalind Franklin Fellowship; European Union and University of Groningen; Short-Term EMBO Fellowship, Grant/Award Number: EMBO7887

Abstract

Aim: A “leaky” gut barrier has been implicated in the initiation and progression of a multitude of diseases, for example, inflammatory bowel disease (IBD), irritable bowel syndrome and celiac disease. Here we show how pro-hormone Chromogranin A (CgA), produced by the enteroendocrine cells, and Catestatin (CST: hCgA₃₅₂₋₃₇₂), the most abundant CgA-derived proteolytic peptide, affect the gut barrier.

Methods: Colon tissues from region-specific CST-knockout (CST-KO) mice, CgA-knockout (CgA-KO) and WT mice were analysed by immunohistochemistry, western blot, ultrastructural and flowcytometry studies. FITC-dextran assays were used to measure intestinal barrier function. Mice were supplemented with CST or CgA fragment pancreastatin (PST: CgA₂₅₀₋₃₀₁). The microbial composition of cecum was determined. CgA and CST levels were measured in blood of IBD patients.

Results: Plasma levels of CST were elevated in IBD patients. CST-KO mice displayed (a) elongated tight, adherens junctions and desmosomes similar to IBD patients, (b) elevated expression of Claudin 2, and (c) gut inflammation. Plasma FITC-dextran measurements showed increased intestinal paracellular permeability in the CST-KO mice. This correlated with a higher ratio of Firmicutes to Bacteroidetes, a dysbiotic

Elke M. Muntjewerff and Kechun Tang shared co-first authorship.

pattern commonly encountered in various diseases. Supplementation of CST-KO mice with recombinant CST restored paracellular permeability and reversed inflammation, whereas CgA-KO mice supplementation with CST and/or PST in CgA-KO mice showed that intestinal paracellular permeability is regulated by the antagonistic roles of these two peptides: CST reduces and PST increases permeability.

Conclusion: The pro-hormone CgA regulates the intestinal paracellular permeability. CST is both necessary and sufficient to reduce permeability and primarily acts by antagonizing PST.

KEYWORDS

Catestatin, chromogranin A, enteroendocrine cells, epithelial tight junctions, gut barrier, inflammatory bowel disease

1 | INTRODUCTION

The intestinal tract harbours 10^3 - 10^{11} bacteria/mL¹ that in aggregate can constitute >1 g of endotoxin.² Endotoxins stimulate immune cells in the lamina propria, which can trigger mucosal inflammation.³ Such inflammation can result in luminal dysbiosis⁴ and gut barrier defects.⁵⁻⁸ The gut barrier is comprised of a surface mucus layer which separates intact bacteria and large particulates from the mucosa⁹ and the colonic epithelium which provides a physical and immunological barrier separating the body from the luminal contents (eg, dietary antigens, a diverse intestinal microbiome and pathogens).¹⁰⁻¹² Mucosal homeostasis is maintained by the delicate and complex interactions between epithelial cells, immune cells and luminal microbiota.¹⁰

The gastrointestinal epithelium not only forms the body's largest interface with the external environment, but also establishes a selectively permeable epithelial barrier; it allows nutrient absorption and waste secretion while preventing the entry of luminal contents. The epithelial barrier is regulated by a series of intercellular junctions between polarized cells: an apical tight junction (TJ), which guards paracellular permeability, the subjacent adherens junction (AJ) and desmosomes; the AJs and desmosomes do not seal the paracellular space but provide essential adhesive and mechanical properties that contribute to paracellular barrier functions.¹¹

The permeability of the barrier is regulated by many factors such as the immune system. For example, tumour necrosis factor (TNF)- α increases the flux of larger molecules, such as proteins and other macromolecules, through the leak pathway, and interleukin (IL)-13 selectively enhances the flux of small molecules and ions via the pore pathway.⁵ TNF- α plays crucial roles in the Caveolin-1-mediated internalization of Occludin (OCLN), which elevates gut permeability. Conversely, overexpression of OCLN alleviates the cytokine-induced increase in gut permeability.⁶ Interferon (IFN)- γ increases gut permeability by reducing the expression of Tight junction protein ZO-1 (TJP1) and OCLN as well

as by modulating actin-myosin cytoskeleton interactions with TJ proteins.⁷ The simultaneous presence of TNF- α and IFN- γ deteriorates intestinal integrity by dissociating TJ proteins.⁸

Here we show that the permeability of the gut barrier is regulated by the pro-hormone Chromogranin A (CgA). CgA is an acidic secretory proprotein¹³ that is abundantly expressed in enteroendocrine cells (EECs) of the gut and serves as a common marker for the EECs of the gut.¹⁴ Originally, CgA was identified as a cellular packaging factor.¹⁵⁻¹⁷ However, the pro-hormone CgA is proteolytically cleaved, both intracellularly as well as extracellularly after its secretion, giving rise to seven bioactive peptides that exert a wide variety of regulatory functions among the metabolic,¹⁸⁻²¹ cardiovascular²²⁻²⁵ and immune systems.²⁶⁻³⁰ Among these bioactive peptide hormones are catestatin (CST: hCgA₃₅₂₋₃₇₂)^{31,32} and pancreastatin (PST: hCgA₂₅₀₋₃₀₁).³³ Blood plasma levels of both intact CgA³⁴⁻³⁶ and CST³⁷ are increased in patients with inflammatory bowel disease (IBD). We show that CST is abundantly generated in the gut. Unexpectedly, we found that CgA regulates the paracellular permeability of the gut via the antagonistic actions of its two peptides, PST and CST; while PST is a pro-inflammatory, pro-obesogenic and anti-insulin peptide²⁰ which loosens the barrier, CST acts as anti-inflammatory, antiobesogenic, anti-microbial and proinsulin peptide^{25,27,29} that appears to be necessary and sufficient to neutralize the actions of PST and tighten the barrier. Using knockout (KO) mice in conjunction with recombinant proteins, we show that CST exerts its actions *via* counteracting PST.

2 | RESULTS

2.1 | CgA is extensively processed to CST

To study the role of CgA and its peptides in the regulation of the gut barrier, we used systemic CgA-KO (deletion of

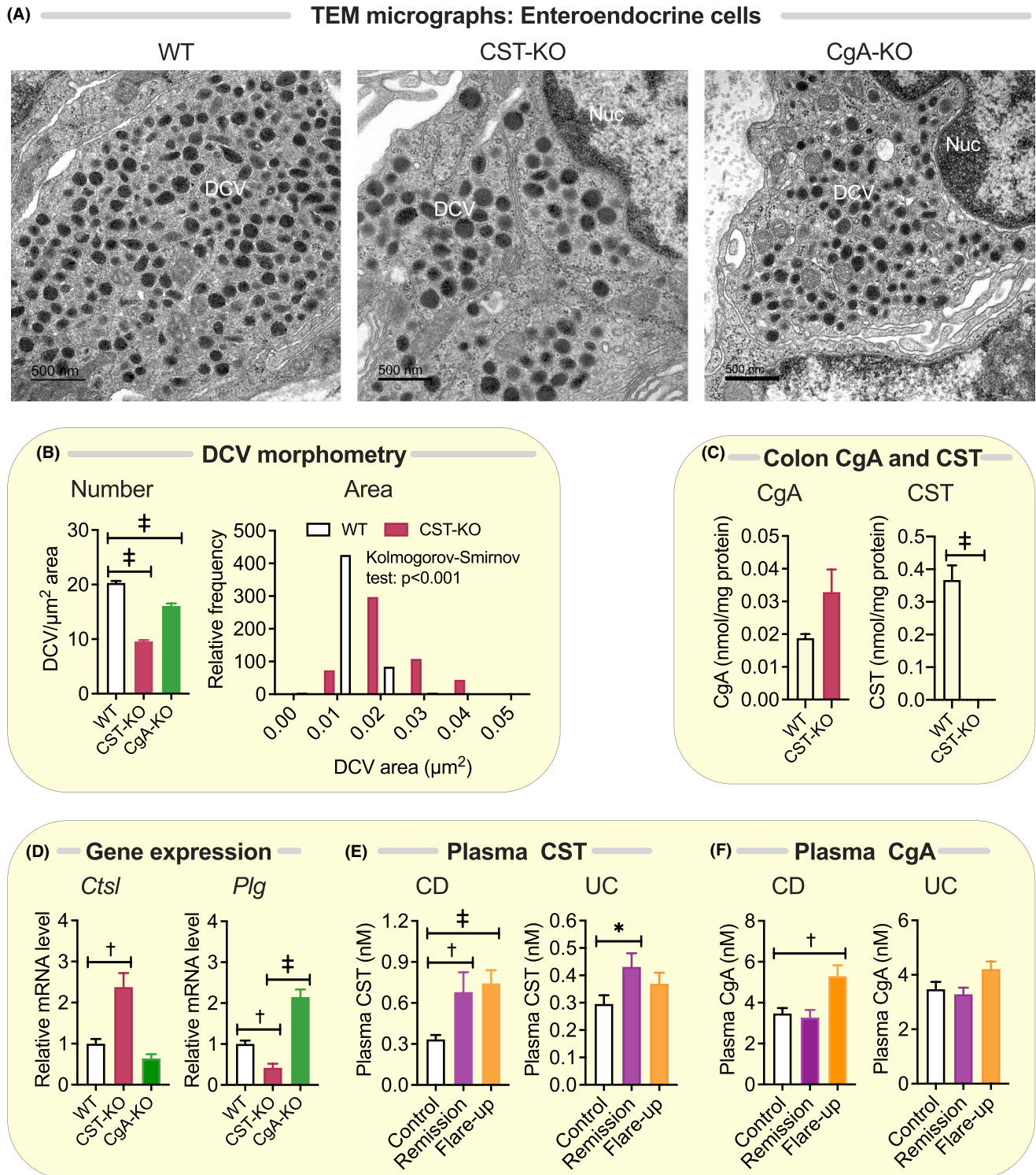


FIGURE 1 CgA is efficiently processed to CST in the colon and CST levels correlate with Crohn's disease activity. A, TEM micrographs ($n = 3$) showing enteroendocrine cell DCV in colon of WT, CgA-KO and CST-KO mice; B, fewer DCV in CgA-KO and CST-KO mice (one-way ANOVA) but enlarged DCV in CST-KO mice and smaller DCV in CgA-KO mice (>500 vesicles from 30 micrographs) (Kolmogorov-Smirnov test). DCV, dense core vesicles; Nuc, nucleus. C, CgA protein and CST peptide levels in colon of WT and CST-KO mice. CgA levels were comparable between WT and CST-KO mice. CST level was markedly higher in WT mice and was undetectable in CST-KO mice ($n = 6$; Welch's t test). D, Expression of proteolytic genes ($n = 7$). *Ctsl* and *Plg* are differentially expressed in colon of CgA-KO and CST-KO mice ($n = 8$; one-way ANOVA). E, CgA and CST levels in EDTA-plasma of healthy donors (Control) and Crohn's disease (CD) and ulcerative colitis (UC) patients ($N = 89$) in remission or flare-up (two-way ANOVA). Ns, not significant; $^{\dagger}P < .01$; $^{\ddagger}P < .001$

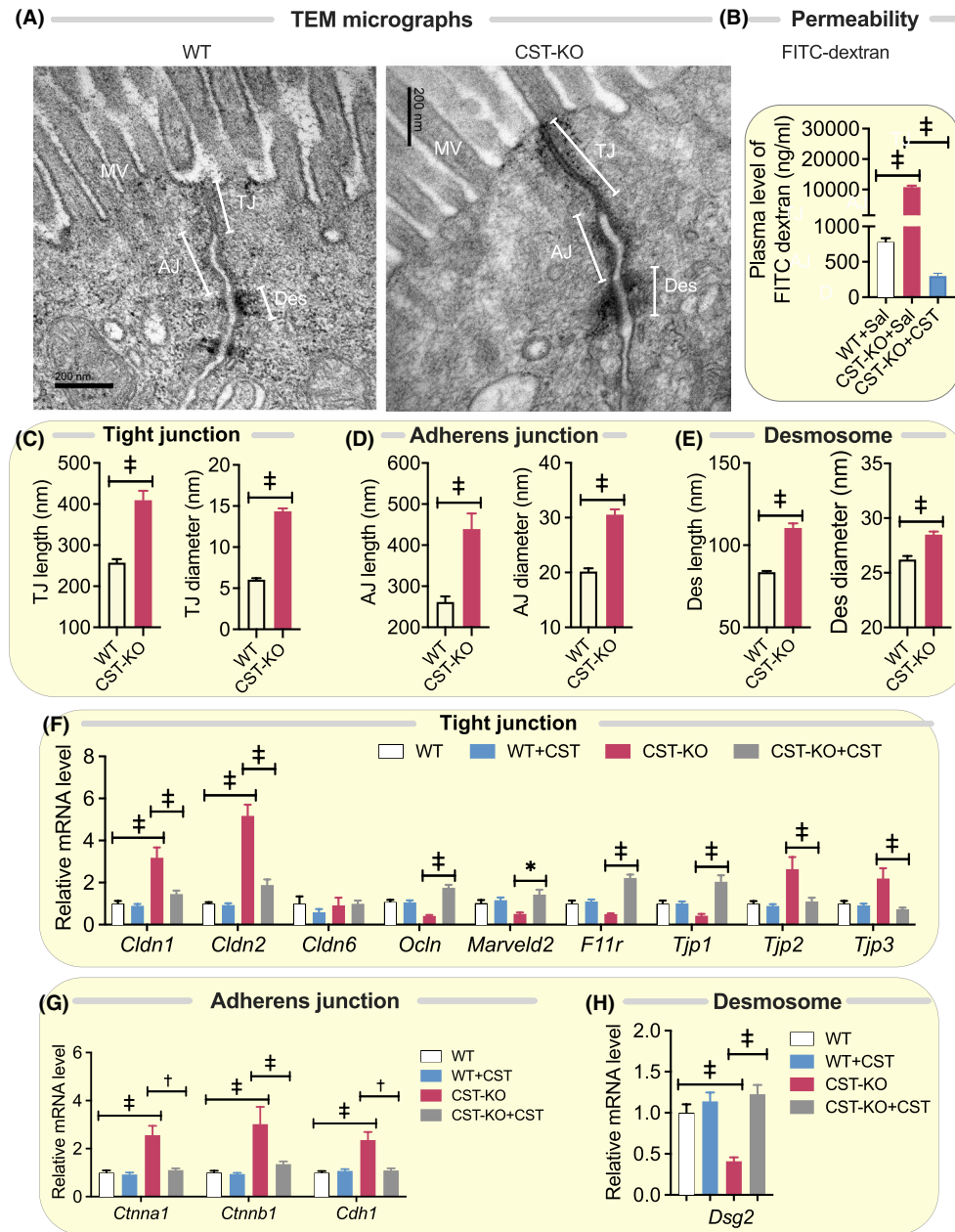


FIGURE 2 Impaired epithelial paracellular barrier function in CST-KO mice. A, TEM micrographs ($n = 3$) showing tight junction (TJ), adherens junction (AJ) and desmosomes (Des). MV, microvillus. B, Increased gut permeability as measured by FITC-dextran level in CST-KO compared to WT mice ($n = 8$; Welch's t test). C-E, Morphometrical analyses ($n = 20$ -54) showing increased length and diameter of TJ (C), AJ (D) and Des (E) in CST-KO mice (Welch's t test). F-H, Differential expression of genes in TJ (*Cldn1*, *Cldn2*, *Cldn6*, *Ocln*, *Marveld2*, *F11r*, *Tjp1*, *Tjp2* and *Tjp3*), AJ (*Ctnna1*, *Ctnnb1* and *Cdh1*) and Des (*Dsg2*) in colon of CST-KO mice compared to WT mice. Supplementation of CST-KO mice with CST reversed the gut permeability and expression of the above genes ($n = 8$; two-way ANOVA or Welch's t test). * $P < .05$; † $P < .01$; ‡ $P < .001$

exon 1 and ~1.5 kbp proximal promoter, thereby completely inactivating the *Chga* allele²² and CST-KO mice (the 63 bp CST domain of CgA was deleted from Exon VII of the *Chga* gene).³⁸ CST-KO mice show low grade inflammation in the heart, pancreas, and liver and have an elevated blood pressure, are obese and suffer from insulin resistance.^{27,38} We analysed the function and morphology of the gut barrier in CST-KO mice. We used transmission electron microscopy (TEM) to

resolve the ultrastructure of EECs and to evaluate the subcellular compartment where hormones are stored and released, that is, dense core vesicles (DCVs). While DCV numbers were reduced in both CgA-KO and CST-KO mice, DCV areas were smaller in CgA-KO mice but larger in CST-KO mice (Figure 1A,B). WT colon showed a lower concentration of CgA (average 0.019 nmol/mg protein) than of CST (average 0.37 nmol/mg protein), indicating extensive processing

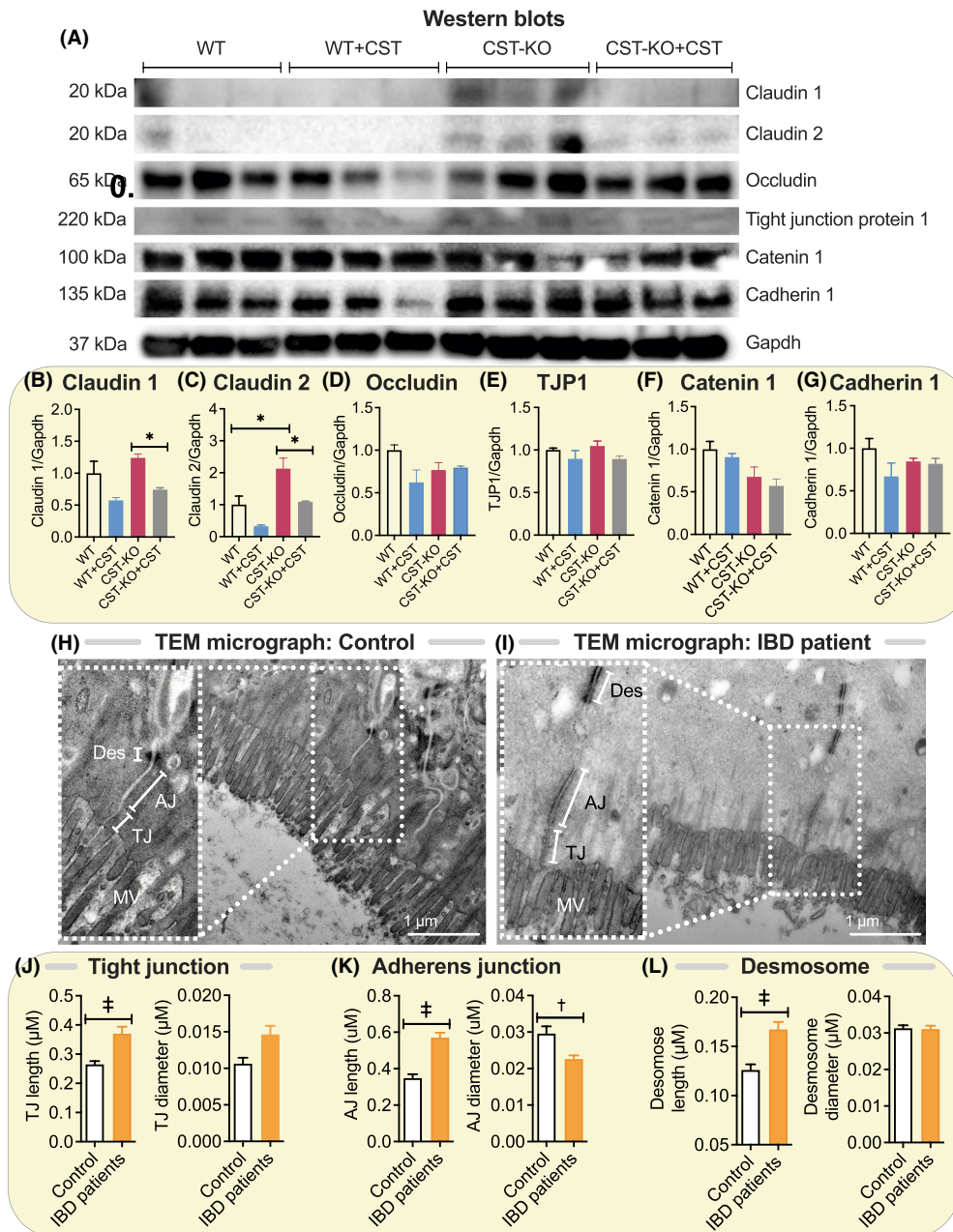


FIGURE 3 Elevated levels of Claudin-2 in colon of CST-KO mice and elongated epithelial junctions in IBD patients. (A) Western blots and (B) densitometric analyses of Claudin-1 (B), Claudin-2 (C), Occludin (D), Tjp1 (E), Catenin 1 (F) and Cadherin 1 (G). H and I, TEM micrographs ($n = 3$) showing tight junction (TJ), adherens junction (AJ) and desmosomes (Des) in healthy control and IBD patients. Microvillus (MV). J-L, Morphometrical analyses ($n = 20-54$) showing increased lengths and diameter of TJ (J), AJ (K) and Des (L) in IBD patients. $*P < .05$; $^{\dagger}P < .01$; $^{\ddagger}P < .001$

of CgA to CST (Figure 1C). As anticipated, in CST-KO mice the levels of CgA in the colon were similar to that in WT mice, but those of CST were undetectable (Figure 1C). Consistent with enhanced processing of CgA, we found increased expression of the proteolytic enzymes Cathepsin L (*Ctsl*, which cleaves CST from CgA) and Plasminogen (*Plg*, the precursor of plasmin, which is involved in CgA processing) in CST-KO and CgA-KO respectively (Figure 1D).^{39,40}

Because the processing of CgA to CST is compromised in several diseases,⁴¹⁻⁴³ we determined plasma CgA

and CST levels in patients with Crohn's disease and with ulcerative colitis, both with active disease and in remission (Figure 1E,F). In line with previous findings,³⁴⁻³⁶ we found higher CgA levels in plasma of patients with active Crohn's disease but not in patients in remission. In contrast, we found higher plasma CST levels in Crohn's disease regardless of disease activity, indicating that the processing of CgA to CST is more efficient in active disease. Patient characteristics are provided in Tables S1 and S2.

2.2 | CST-KO mice have a “leaky” gut

Ultrastructural evaluation of the gut epithelium revealed that the TJs, AJs and desmosomes are significantly different in CST-KO mice compared to wild-type (WT): the TJs, AJs and desmosomes were elongated, as also observed in IBD patients (Figures 2A,C-E and 3H-L). We determined whether this altered morphology was caused by an altered expression of proteins involved in these epithelial junctions. Gene expression studies showed a trend towards lower mRNA expression of multiple TJ-markers such as Occludin (*Ocln*), MARVEL domain-containing protein 2 (*Marvel2*, also called Tricellulin), Junctional adhesion molecule A (JAM-A; *F11r*) Tight junction protein ZO-1 (*Tjp1*)⁴⁴ and the desmosomal protein Desmoglein 2 (*Dsg2*), which is required for maintenance of intestinal barrier function.⁴⁵ We observed concomitant elevated mRNA expression of the genes coding for TJ components Claudin 1 and 2 (*Cldn1* and *Cldn2*), TJ protein ZO-2 and 3 (*Tjp2* and *Tjp3*), and AJ genes coding for alpha-E-Catenin (*Cttna1*), Cadherin-associated protein (*Cttnb1*) and Cadherin 1 (*Cdh1*) (Figure 2F–H). Primer sequences are provided in Table S3. For Occludin, ZO-1, alpha-E-Catenin, Cadherin 1, Claudin 1, we did not observe significantly altered protein levels (Figure 3A–F). However, we did find expression at both the mRNA and protein levels of *Cldn2* (Figures 2F and 3A,G), a specific claudin that is known to increase the paracellular flux of cations and water through the pore pathway.⁴⁶

In order to assess the functional consequence of the altered cellular junctions, we determined the flux through the leak pathway, which is responsible for the paracellular movement of larger molecules, including microbial proteins and other macromolecules. Compared to WT mice, we observed a more than 10-fold increase in leakage of plasma FITC-dextran (4 kDa) in the CST-KO mice (Figure 2B). This confirms that the intestine in CST-KO mice has a strongly diminished paracellular barrier via the leak pathway, although the large magnitude of leakage might even suggest direct epithelial damage.

2.3 | CST-KO mice and IBD patients show comparable ultrastructural changes in tight junctions, adherens junctions and desmosomes

Ultrastructural analyses of colonic mucosa revealed increased lengths of TJ, AJ, and desmosomes in IBD patients compared to healthy controls (Figure 3H-L). Unlike CST-KO mice, IBD patients displayed a decrease in AJ diameter (Figure 3H,K and I).

2.4 | The leaky gut in CST-KO mice is accompanied by mucosal inflammation and dysbiosis

Because inflammation regulates the epithelial cellular junctions⁵⁻⁸ and an increased gut permeability is often associated with mucosal inflammation, we investigated the immune cell populations in the colons of CST-KO mice by histochemical analysis (Figure 4A-C). Indeed, the colon of CST-KO mice displayed signs of mucosal inflammation, such as elevated immune cell infiltration (Figure 4D,E), increased fibrosis (Figure 5D,E) and increased apoptosis (Figure 6A). In addition, there was increased abundance of macrophages (CD45⁺11b⁺Emr1⁺) and helper CD4⁺ T cells in the colon of CST-KO mice as confirmed by flow cytometry (Figure 4F). Moreover CST-KO mice showed increased expression of the following proinflammatory genes: TNF- α (*Tnfa*), IFN- γ (*Ifng*), Chemokine CXC motif ligand 1 (*Cxcl1* aka *Kc/Gro1*), Chemokine CC motif ligand 2 (*Ccl2* aka *Mcp1*), Egg-like module-containing mucin-like hormone receptor 1 (*Emr1* aka *F4/80*), Integrin alpha-M (*Itgam* aka *Cd11b*) and Integrin alpha-X (*Itgax* aka *Cd11c*) (Figure 4G). Increased expression of *Tnfa*, *Ifng*, *Cxcl1* and *Ccl2* genes correlated with increased protein levels (Figure 5A). Upregulation of proinflammatory cytokines is in line with prior work demonstrating a positive correlation of IFN- γ ⁴⁷ and TNF- α ⁴⁴ with intestinal leakiness. The decreased expression of anti-inflammatory cytokines, such as interleukin 4 (*Il4*) and interleukin 10 (*Il10*), in CST-KO mice is also in congruence with the reported role of anti-inflammatory cytokines in gut permeability (Figure 5C).⁴⁸ The decreased *Il10* mRNA levels correlated with a decreased protein level of IL-10 (Figure 5C). Furthermore, the expression of *S100a9* gene (forming Calprotectin in complex with S100a8) was increased in colon of CST-KO mice and Calprotectin protein levels were increased in plasma, colon and faeces of CST-KO mice (Figure 5B); increased Calprotectin, a protein secreted by activated neutrophils and macrophages, has been shown to be associated with increased intestinal permeability.⁴⁹ The increased inflammation in the gut of CST-KO mice is consistent with the known anti-inflammatory roles of CST^{29,50} and with our previous observation of low-grade systemic inflammation in the CST-KO mice.²⁷

Because a leaky gut may either cause or be the consequence of altered luminal microbes,⁵¹ we investigated whether the microbial population in CST-KO mice was altered. We found that the microbiome in CST-KO mice was indeed quite different in composition than its WT littermates (Figures 6B-E and 7). Most prominently, CST-KO mice showed a higher ratio of Firmicutes to Bacteroidetes (Figure 6C-E), which is opposite to the decreased ratio observed in WT mice intrarectally infused with CST,⁵² and supports the idea that a low ratio of Firmicutes to Bacteroidetes could be beneficial to dampen intestinal inflammation.⁵²

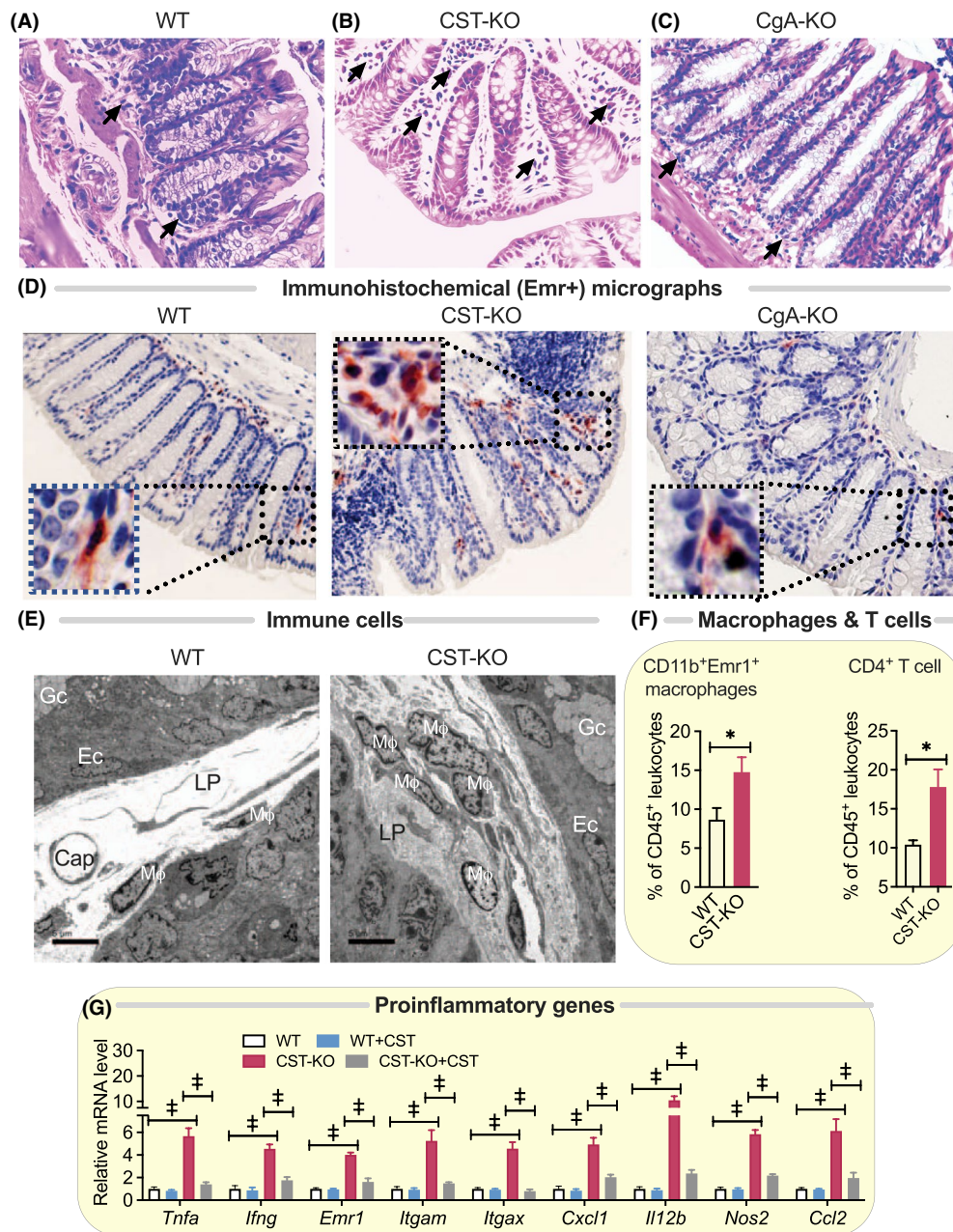


FIGURE 4 Increased infiltration of immune cells in colon of CST-KO mice. A-C, haematoxylin and eosin-stained histological micrographs of colon in WT (A), CST-KO (B), and CgA-KO (C) mice. Arrows indicate immune cells. D, Immunohistological micrographs showing increased infiltration of Emr⁺ cells in CST-KO mice. E, TEM micrographs (n = 3) showing increased number of immune cells in colon of CST-KO mice. Mφ, macrophage; Cap, capillary; Ec, enterocytes; Gc, goblet cells; LP, lamina propria. F, Flow cytometry study (n = 5-10) shows increased number of macrophages (CD45⁺CD11b⁺Emr1⁺) and T cells (CD45⁺CD4⁺) in colon of CST-KO mice (n = 5-10; Welch's *t* test). G, Increased expression of proinflammatory genes (*Tnfa*, *Ifng*, *Cxcl1*, *Ccl2*, *Emr1*, *Il12b*, *Nos2*, *Itgam* and *Itgax*), which returned to WT levels after treatment with CST (n = 8; two-way ANOVA). **P* < .05; †*P* < .01; ‡*P* < .001

That the leaky gut of CST-KO mice is inflamed and harbours dysbiotic luminal contents implies that CST is required for maintaining gut barrier integrity and preventing dysbiosis and gut inflammation. This is important because a “leaky gut”,⁵³ dysbiosis⁵⁴ and hyperactivated immunity⁵⁵ are all well known to play a role in IBD. It is also consistent with others' observation that administration of exogenous CST can ameliorate colitis in mice.⁵⁵

2.5 | CST is sufficient to tighten the leaky gut barrier in CST-KO mice and reduce inflammation

To test whether CST is sufficient to regulate gut permeability, we supplemented CST-KO mice with recombinant CST (intraperitoneal injections of 2 μg/g body weight once daily for at least 15 days), which reversed paracellular

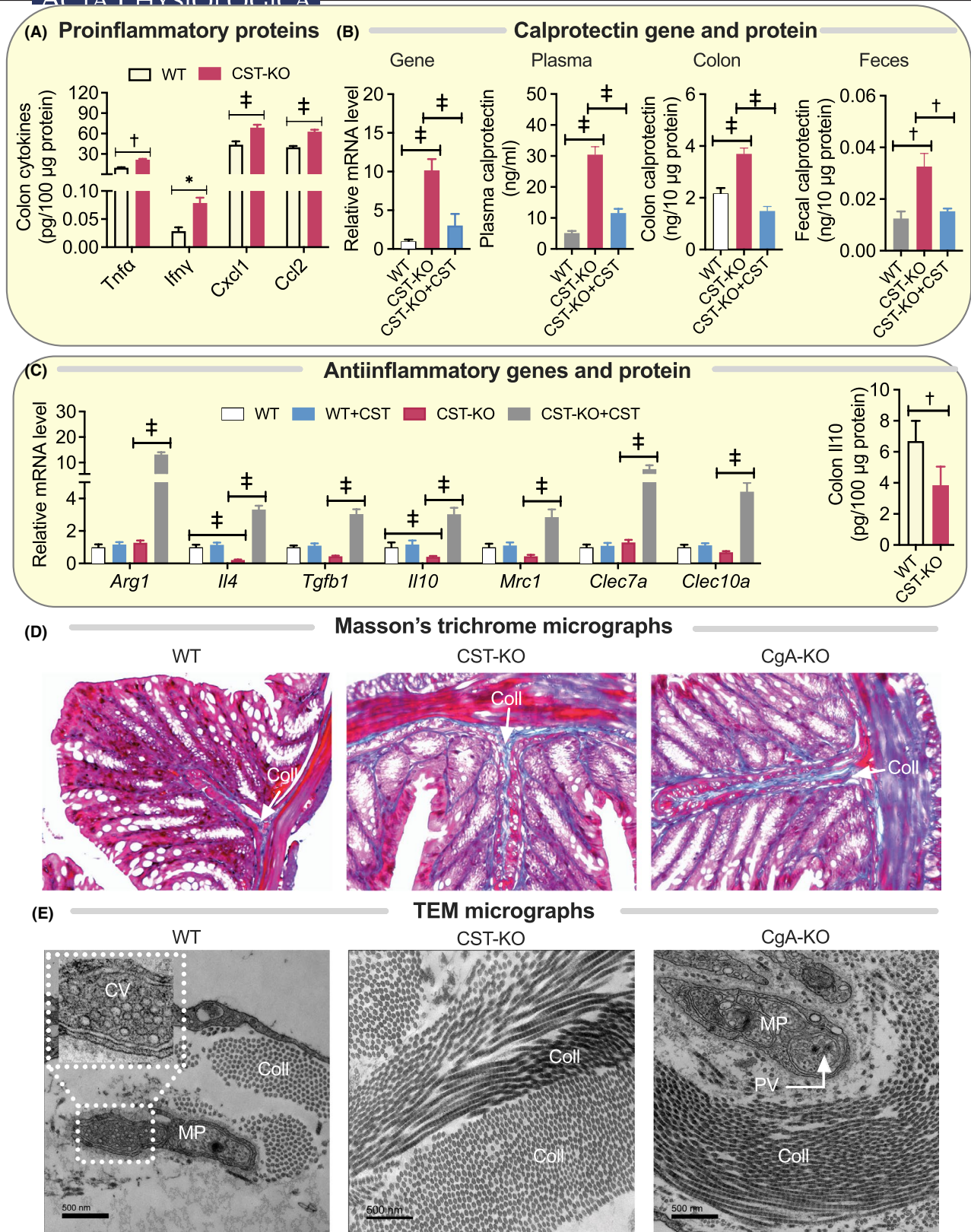


FIGURE 5 Elevated levels of pro-inflammatory proteins and fibrosis in colon of CST-KO mice. **A**, Increased expression of proinflammatory proteins (*Tnfa*, *Ifny*, *Cxcl1* and *Ccl2*) in colon of CST-KO mice ($n = 8$; two-way ANOVA). **B**, Increased expression of proinflammatory Calprotectin gene *s100A9* in colon and Calprotectin protein in plasma, colon and faeces of CST-KO mice, which were reversed upon administration of CST for 15 d ($n = 5$; one-way ANOVA). **C**, Decreased expression of anti-inflammatory genes (*Arg1*, *Il4*, *Tgfb1*, *Il10*, *Mrc1*, *Clec7a* and *Clec10a*) ($n = 8$; two-way ANOVA), and anti-inflammatory protein (Il10) ($n = 8$; Welch's *t* test) in colon of CST-KO mice. CST treatment increased expression of anti-inflammatory genes in CST-KO mice. **D**, Masson's trichrome-stained histological micrographs showing increased fibrosis in CST-KO and CgA-KO colon. **E**, TEM micrographs showing increased presence of collagen fibers in CST-KO and CgA-KO mice. Coll, collagen; CV, clear cholinergic vesicles; MP, Meissner's plexus; PV, dense core peptidergic vesicles. * $P < .05$; ** $P < .01$; *** $P < .001$

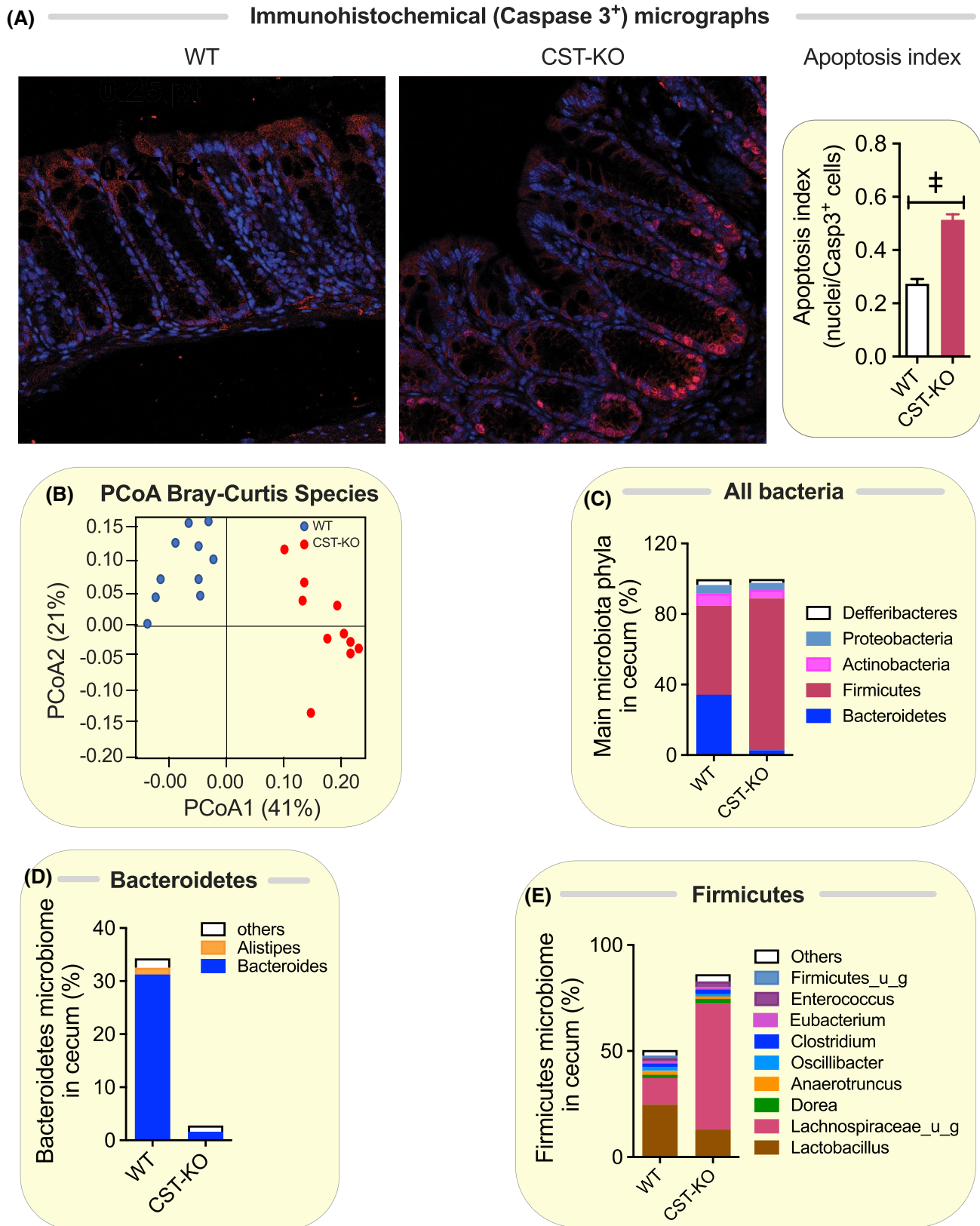


FIGURE 6 Increased apoptosis and ratio of Firmicutes to Bacteroidetes in gut of CST-KO mice. A, increased numbers of Caspase-3 positive apoptotic cells in colon of CST-KO mice. B, Principal CoordinatE Analysis (PCoA) of microbiome data using Bray-Curtis distance of species composition and abundance in individual WT (blue) and CST-KO (red) mice. C-E, Microbiota composition of cecum of WT and CST-KO mice for main bacteria phyla (C) and the geni within the Bacteroidetes (D) and Firmicutes (E)

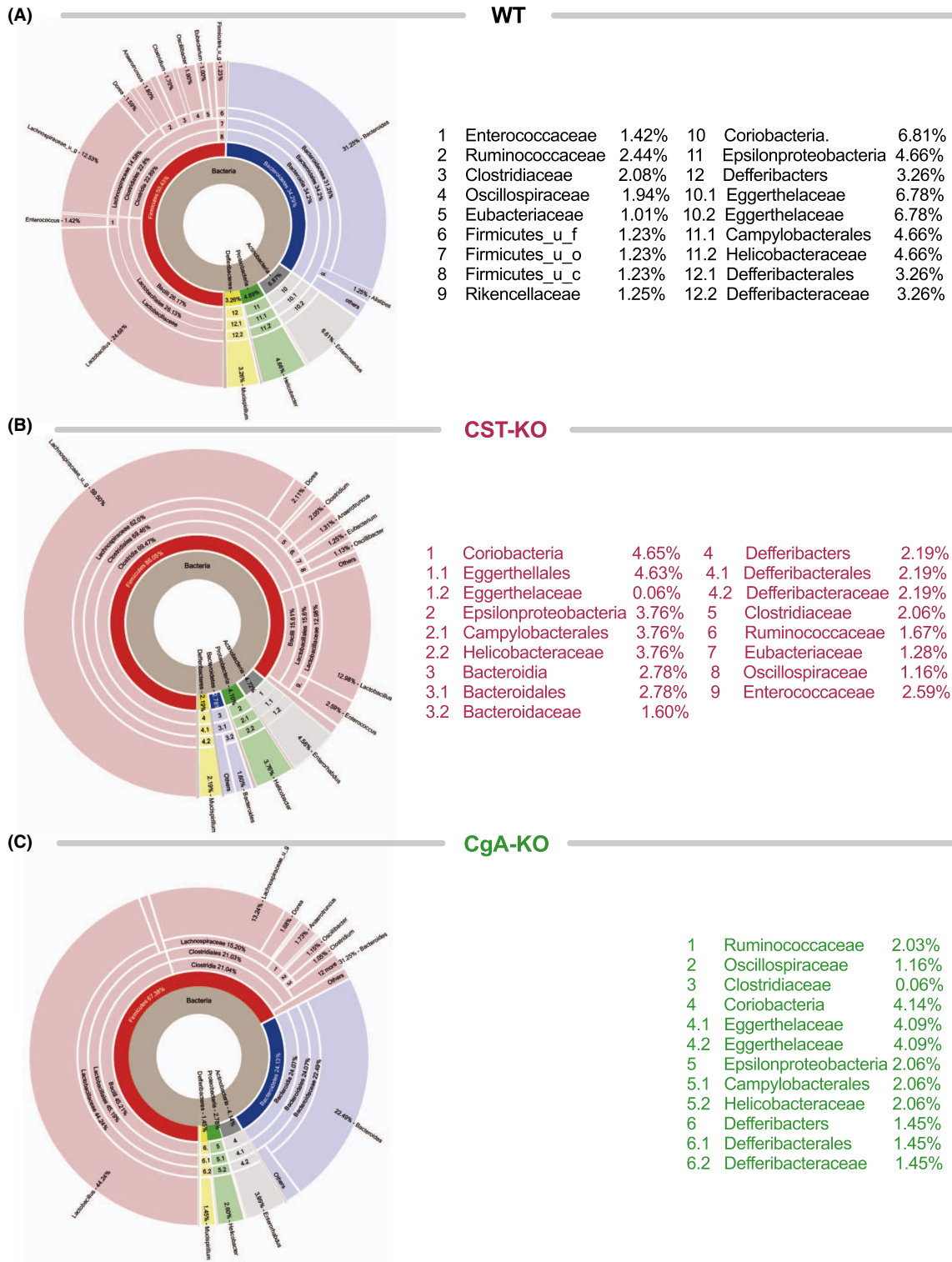


FIGURE 7 Detailed microbial composition of WT, CST-KO and CgA-KO mice. Graphs show complete microbiota composition in cecum of WT (A), CST-KO (B) and CgA-KO (C) mice. Circles from inside to outside show kingdom, phylum, class, order, family and genus

leakiness of FITC-dextran and the associated abnormalities such as: (a) reduced plasma FITC-dextran even lower than WT level (Figure 2B), (b) increased mRNA expression of *Ocln*, *Marveld2*, *F11r*, *Tjp1* and *Dsg2* (Figure 2F,H), (c) decreased mRNA expression of *Cldn1*, *Cldn2*, *Tjp2*, *Tjp3*, *Ctnn1*, *Ctnnb1* and *Cdh1*, as well as increased protein

expression of Claudin-2 (Figures 2F,G and 3A,C), (d) decreased mRNA expression of proinflammatory genes (*Tnfa*, *Ifng*, *Cxcl1*, *Ccl2*, *Emr1*, *Il12b*, *Nos2*, *Itgam* and *Itgax*) (Figure 4G), (e) increased expression of anti-inflammatory genes (*Arg1*, *Il4*, *Tgfb1*, *Il10*, *Mrc1*, *Clec7a* and *Clec10a*) (Figure 5C), (f) decreased expression of Calprotectin gene

(subunit *SI00a9*) and protein levels (Figure 5B). These findings demonstrate that CST reduces intestinal inflammation, and that CST is not only required for the integrity of the paracellular gut barrier, but is also sufficient to maintain the integrity of this barrier during homeostasis.

2.6 | The paracellular permeability of the gut is intact in CgA-KO mice

Next, we carried out the gut barrier studies in CgA-KO mice, which not only lack CST, but also lack all other peptides derived from CgA. Ultrastructural studies showed no structural changes in TJ, AJ and desmosomes in CgA-KO mice compared to WT mice (Figure 8A). To our surprise, we found that despite the absence of CST in these mice, the gut permeability for FITC-dextran was not increased (Figure 8B); if anything, the paracellular barrier was even tighter than WT control mice. This decreased permeability was not accompanied by changes in CgA-KO mice in genes coding for components of TJ, AJ and desmosomes, except that *Ocln* and *Dsg2* gene expression were decreased in CgA-KO mice compared to WT mice (Figure 8C). Likewise, proinflammatory gene and protein expressions were not affected in CgA-KO mice (Figure 8D-E). In line with this, histology and EM revealed some fibrosis, but no excessive immune cell infiltration in the colon of CgA-KO mice (Figure 5D,E). In contrast to the CST-KO mice, the CgA-KO mice even showed increased colonic expression of anti-inflammatory genes and proteins (Figure 8F-G). The decreased colon levels of Calprotectin were also consistent with decreased gut permeability (Figure 8H). Compared to CST-KO mice, Firmicutes and Bacteroidetes bacteria populations in CgA-KO mice were more comparable to WT mice (Figures 7 and 9A).

These findings suggest that CST is not essential in the absence of CgA. Because a leaky and inflamed gut was seen in the CST-KO mice which specifically lack the proteolytic fragment of CST, but not in CgA-KO mice which lack CST and all other peptides that are generated proteolytically from CgA, these findings raised the possibility that CST may be required to antagonize the actions of some other peptide hormone that is also a product of CgA.

2.7 | Gut permeability is regulated by the antagonistic effects of two CgA peptides: CST and Pancreastatin (PST)

Among the various proteolytic peptides, we hypothesized that CST could be acting to balance the impact of PST, another peptide fragment of CgA (Figure 9B). This hypothesis was guided by prior work⁴³ alluding to PST's

deleterious impact on the gut mucosa, causing macrophage infiltration and inflammation. To test the nature of contribution of PST and CST on the gut paracellular barrier function, we supplemented the CgA-KO mice with either CST alone (2 µg/g body weight for 15 days), or PST alone (2 µg/g body weight for 15 days), or both PST and CST co-administered at equimolar ratio for 15 days. CST alone did not change leakiness of FITC-dextran in CgA-KO mice (Figure 9C).

By contrast, PST alone increased the leakiness in CgA-KO mice and this leakiness was markedly reduced when the CgA-KO mice received both PST and CST at equimolar concentration (Figure 9C). These findings indicate that PST increases the paracellular gut permeability, and that CST antagonizes this action. Together, these data lead us to propose a working model (Figure 9D) in which the intestinal epithelial paracellular barrier is finetuned by the EECs via a major gut hormone, CgA. Our data show that CgA is proteolytically processed into two peptides, CST and PST, which tighten and loosen the gut barrier respectively.

3 | DISCUSSION

The major finding in this work is the discovery of a molecular mechanism that involves a major EEC-derived gut hormone that has a balanced action on the paracellular gut barrier; two hormone derivatives of CgA, that is, CST and PST, which either tighten or loosen the barrier respectively. Because CgA-KO mice had unimpaired leakage of FITC-dextran, which was increased by exogenous administration of PST but not reduced by exogenous CST alone, the findings also indicate that the barrier-homeostatic mechanism(s) is contained within and converge at a molecular level on the prohormone CgA and its processing into counteracting peptide hormones. These findings are important because CST is a major peptide hormone in EEC which is proteolytically produced from CgA by proprotein convertase 1 (PC1),⁵⁵ cathepsin L,⁵⁶ plasmin⁴⁰ and kallikrein.⁵⁷ Its abundance in the gut suggests that the permeability of the gut barrier is regulated by CST.

CgA is unique in having peptide domains that antagonize several functions including inflammation (CST suppresses while PST promotes), obesity (CST inhibits while PST stimulates) and sensitivity to insulin (CST increases while PST diminishes).^{20,27,58} Since CgA-KO mice lack both CST and PST, and we observed increased permeability in CST-KO mice and decreased permeability in CgA-KO mice, we reasoned that these opposing phenotypes are probably caused by the lack of PST in the CgA-KO mice. Indeed, the increased permeability in PST-treated CgA-KO mice and its reversal by co-treatments of PST and CST lead us to conclude that

CST promotes the epithelial paracellular barrier function by counteracting PST. Nevertheless, the baseline gut permeability in CST-KO mice was higher than in CgA-KO mice

supplemented with PST. This might suggest that there are other cleavage fragments of CgA that regulate the intestinal permeability or that the effects cannot be completely reversed.

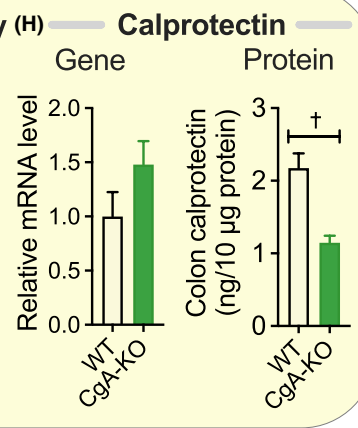
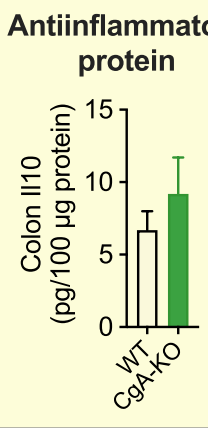
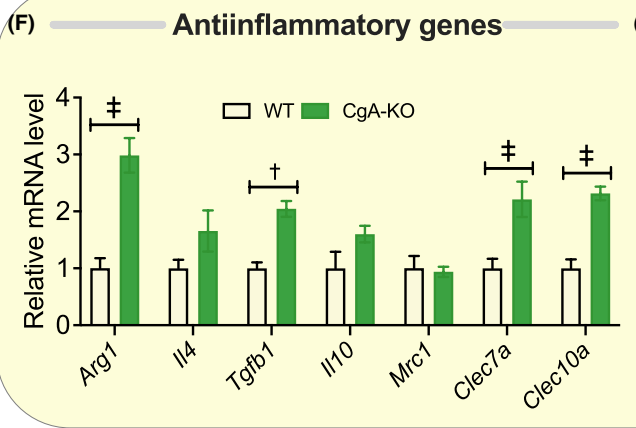
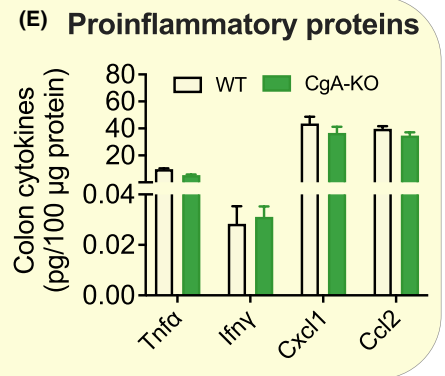
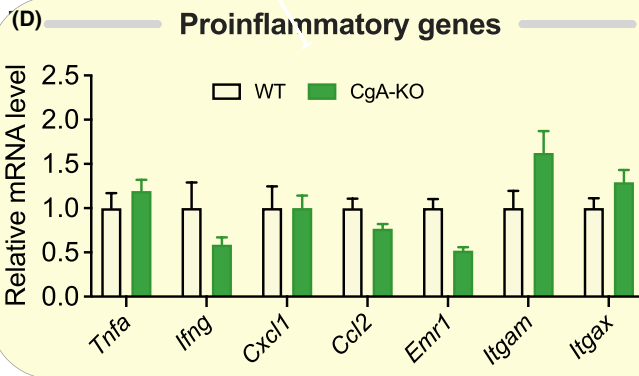
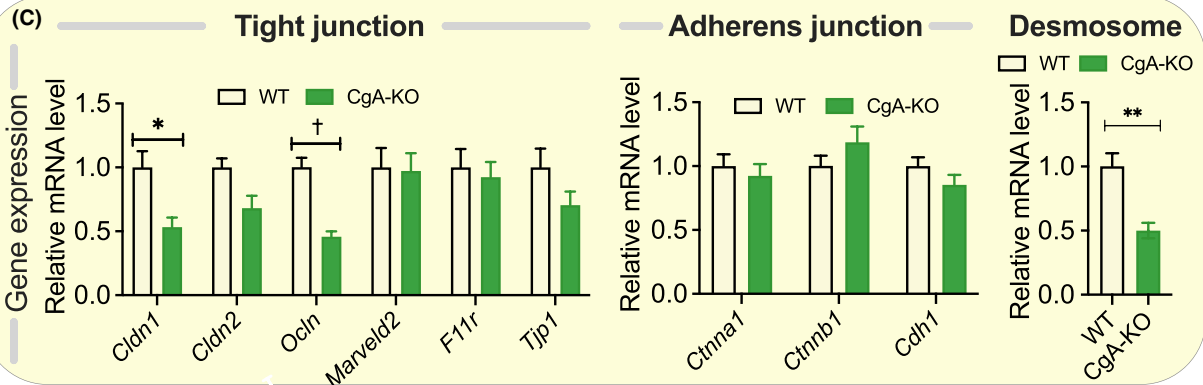
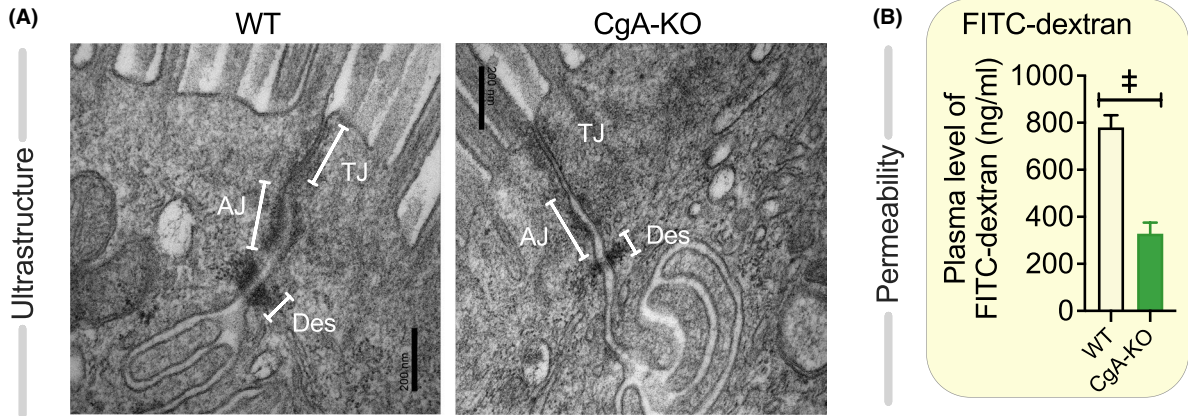


FIGURE 8 Increased epithelial paracellular barrier function and lower inflammation in CgA-KO mice. A, Electron microscopy micrographs of colon of WT and CgA-KO mice. TJ: tight junction. AJ: adherens junction. Des: desmosomes. B, Gut permeability as measured by FITC-Dextran plasma level in WT and CgA-KO mice ($n = 7$; Welch's t test). C, Relative mRNA expression of genes in tight junction (*Cldn2*, *Ocln*, *Marveld2*, *Fllr* and *Tjp1*) ($n = 8$, two-way ANOVA), adherens junction (*Ctnna1*, *Ctnnb1* and *Cdh1*) ($n = 8$; two-way ANOVA), and desmosome (*Dsg2*) ($n = 8$; Welch's t test) in colon of WT and CgA-KO mice. Comparable expression of (D) proinflammatory genes (*Tnfa*, *Ifng*, *Cxcl1*, *Ccl2*, *Emr1*, *Itgam* and *Itgax*), and (E) proinflammatory proteins (Tnf α , Ifn γ , Cxcl1 and Ccl2) in colon of WT and CgA-KO mice ($n = 8$, two-way ANOVA). Increased expression of (F) anti-inflammatory genes (*Arg1*, *Tgfb1*, *Clec7a* and *Clec10a*) and comparable expression of anti-inflammatory genes (*Il4*, *Il10* and *Mrc1*), and (G) anti-inflammatory protein (Il10) in colon of WT and CgA-KO mice ($n = 8$; two-way ANOVA or Welch's t test). H, Comparable expression of *s100a9* gene and decreased expression of calprotectin protein in CgA-KO colon ($n = 5$; Welch's t test). [†] $P < .01$; [‡] $P < .001$

While PST exerts deleterious impact on the gut mucosa, causing macrophage infiltration and inflammation,⁵⁹ we found that lack of CST caused an increased expression of proinflammatory genes and proteins and treatment of CST-KO mice with CST reversed expression of those genes and proteins. These findings are in line with the anti-inflammatory roles of CST^{27,29} and with the low-grade systemic inflammation present in the CST-KO mice.^{27,29} Our findings are also in congruence with the existing literature which showed increased TJ permeability in presence of increased proinflammatory cytokines such as TNF- α , IL-1 β and IFN- γ .⁶⁰ A reduced gut barrier function might facilitate the leakage of microbial components such as lipopolysaccharide (LPS) and peptidoglycan (PGN) from the lumen of the gut into the tissues, where they can bind to pattern recognition receptors and activate the immune system. In turn, the increased inflammation can result in further leakage of the gut. For instance, myosin light chain kinase (MLCK) plays critical roles in cytokine-mediated TJ regulation by disrupting the interaction between TJ proteins and the actin-myosin cytoskeleton⁶¹ leading to damage of the TJ scaffold, which is crucial for the maintenance of barrier integrity.⁶¹ Inflammatory cytokine-induced intestinal barrier loss is also believed to be due to endocytosis of TJ proteins, which also requires MLCK transcription and activity at the TJ,⁶ although we did not observe decreased protein levels of TJ proteins in the colon of CST-KO mice. In addition to the above mechanisms, TNF- α suppresses TJ barrier function by decreasing expression of TJP1 protein, increasing expression of Claudin-2, and activating the NF- κ B pathway.⁶² IL-6 also increases expression of Claudin-2.⁶³ In line with this, we observed elevated levels of Claudin-2 in the colon of CST-KO mice.

In addition to these indirect effects on TJ protein expression and structure via the immune system, it might also be possible that CgA and/or its cleavage products exert direct effects on the epithelial cells and thereby more directly regulate the TJs. To investigate this, it will be interesting to perform in vitro experiments, for example, epithelial monolayers in perfusion chambers co-cultured with or without immune cells.⁶⁴

An interesting question is how CST and PST affect the AJs and desmosomes. Not only TJ components, but also

desmosome and AJ components are altered in CST-KO mice and these changes are reversible by administration of exogenous CST. It might be possible that the AJs and/or desmosomes are part of a feedback mechanism to compensate the altered TJ structure. Previously, by using Dsg2-KO mice, desmosomes have been shown to regulate the intestinal barrier.⁴⁵ Moreover, Dsg2 modulates the production of glial cell-derived neurotrophic factor (GDNF) in inflammatory bowel disease patients.⁶⁵ Therefore, a possible scenario is that CgA-derived peptides regulate the release of GDNF from enteric glial cells in the gut wall, which in turn affects the epithelial junctions.

The present study unequivocally demonstrates that CST is a key regulator of paracellular gut permeability since the absence of CST (CST-KO) is accompanied by dysbiosis, increased gut permeability for FITC-dextran, increased infiltration of macrophages and CD4⁺ T cells, and higher local inflammatory gene and protein expression with the substitution of CST-KO mice with CST reversing many of the above abnormalities. Do gut hormones simulate the actions of CST? While Cholecystokinin (CCK) decreases mucosal production of proinflammatory cytokines induced by LPS and increases the expression of seal forming TJ proteins (OCLN, Claudins and JAM-A),⁶⁶ Ghrelin ameliorates sepsis-induced gut barrier dysfunction by activation of vagus nerve via central ghrelin receptors⁵³ as well as by decreasing production of TNF- α and IL-6.⁶⁷ Glucagon-like peptide 1 (GLP-1) has also been shown to decrease inflammation of enterocytes.⁶⁸ Vasoactive intestinal peptide, a neuropeptide found in lymphocytes,⁶⁹ mast cells,⁷⁰ and enteric neurons of the gastrointestinal tract regulates both epithelial homeostasis⁷¹ and intestinal permeability.⁷² The multitude of effects of CST on gut physiology and their recapitulation by these well-investigated gut hormones establishes CST as an important gastrointestinal peptide hormone.

CST-KO mice (loss of barrier integrity) are hypertensive and insulin-resistant on normal chow diet^{27,38} and CgA-KO mice (intact barrier integrity) are also hypertensive but are supersensitive to insulin in both normal chow and on high fat diet.^{18,20} Could metabolic endotoxemia explain the above phenotypes? Besides gastrointestinal peptide hormones and neuropeptides, TJ homeostasis is altered by proinflammatory cytokines, pathogenic bacteria, and pathological

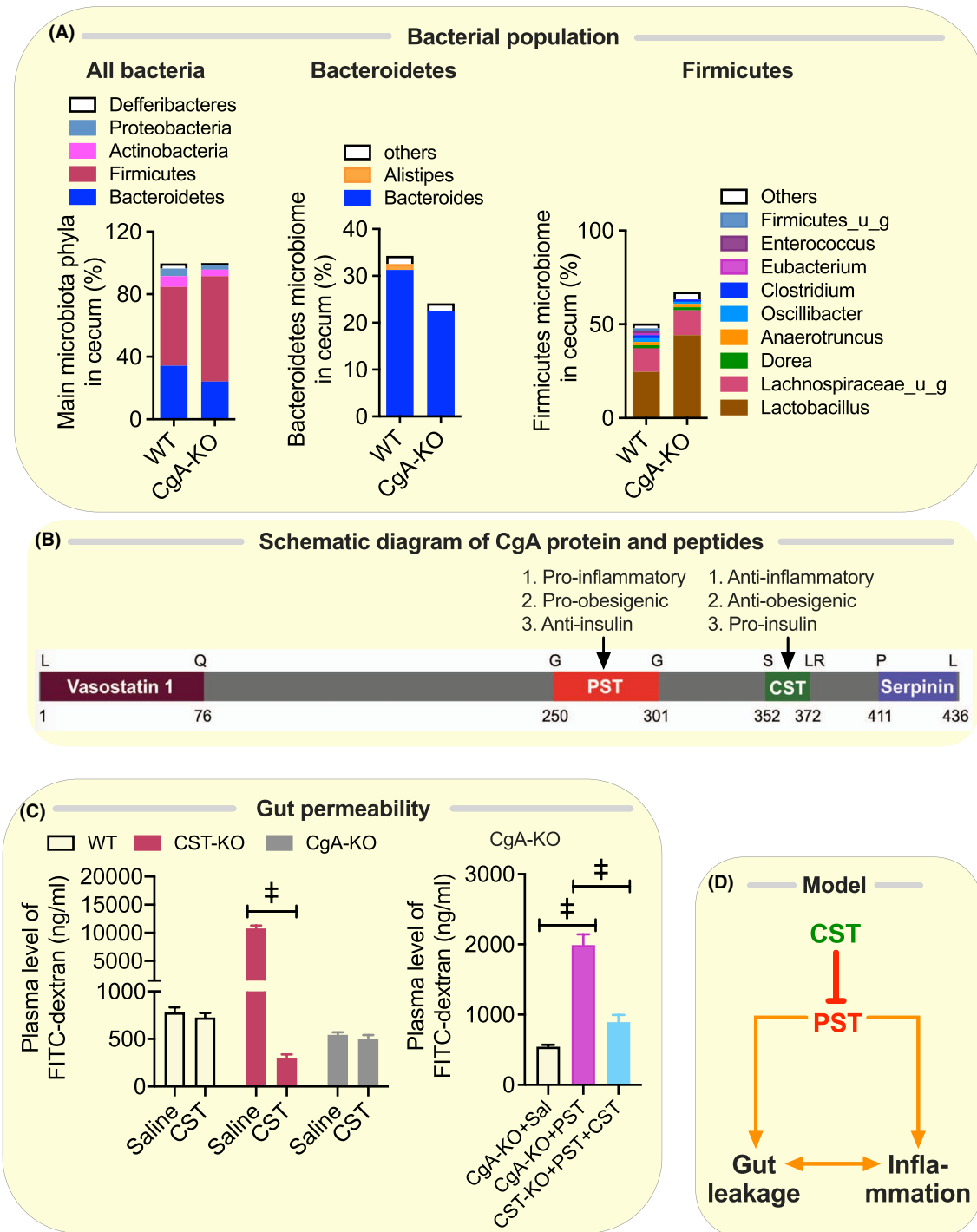


FIGURE 9 Altered microbiome composition in CgA-KO mice and CST and PST oppositely regulate gut permeability. A, Microbiota composition of cecum of WT and CgA-KO mice for main bacteria phyla and the geni within the Bacteroidetes and Firmicutes. B, Scheme of CgA indicating the positions of the peptide products vasostatin 1, PST, CST and serpinin. C, Gut permeability as measured by FITC-Dextran plasma levels in WT, CST-KO and CgA-KO mice treated with saline or CST ($n = 8$; two-way ANOVA) and in CgA-KO mice treated with PST or a combination of PST and CST ($n = 8$; one-way ANOVA). D, Model of gut barrier regulation by CST and PST. $^{\#}P < .001$

conditions like insulin resistance and obesity. Firmicutes (eg, *Lactobacillus*, *Clostridium* and *Enterococcus*) and Bacteroidetes (eg, *Bacteroides*) constitute the major bacterial phyla in the gut.⁷³ Toxicogenic bacteria cause diarrhoea via

increased ion permeability of the pore pathway,⁵¹ but gut microbes might also affect the leak pathway. Enteric pathogenic bacteria such as *Escherichia coli* and *Salmonella typhimurium* alter the intestinal epithelial TJ barrier and cause intestinal

inflammation.⁷⁴ LPS alters expression and localization of TJ proteins such as TJP1 and OCLN.⁷⁵ Therefore, it would be interesting to study whether the systemic LPS levels support the observed dysbiosis-related loss of gut barrier in the CST-KO mice. Since high fat diet-induced insulin-resistant mice and patients with obesity or diabetes display elevated levels of Firmicutes and Proteobacteria compared to the beneficial phylum Bacteroidetes,⁷⁶ it is conceivable that dysbiosis (ie, increased Firmicutes and decreased Bacteroidetes) in CST-KO mice is due to their resistance to insulin. This is further supported by the fact that *Akkermansia muciniphila*, which regulates intestinal barrier integrity, is less abundant in diabetic individuals.⁷⁷ Furthermore, the daily administration of *A muciniphila* is known to mitigate high fat-induced gut barrier dysfunction.⁷⁸ Conversely, metabolic endotoxemia, resulting from the loss of barrier integrity, contributes to insulin resistance and obesity.^{76,79} The intact paracellular barrier function in CgA-KO mice could thus be due to their heightened sensitivity to insulin.

Human calprotectin, a 24 kDa dimer, is formed by S100A8 and S100A9 monomers and released from neutrophils and monocytes. In fact, this calprotectin complex constitutes up to 60% of the soluble proteins in the cytosol of neutrophils⁸⁰ and faecal calprotectin levels serve as a marker of intestinal inflammation.^{81,82} Because of the positive correlation between calprotectin concentration in gut lavage fluid and intestinal permeability,⁸³ calprotectin levels are also used to assess intestinal permeability. Increased calprotectin levels have been reported to increase intestinal permeability.⁴⁹ Therefore, increased gene and protein expressions in the colon of CST-KO mice are in line with the increased permeability in CST-KO mice.

Elevated plasma CST levels in patients suffering from Crohn's disease both in disease remission and flare-up as compared to elevated precursor CgA in Crohn's disease flare-ups only suggests that while CgA is generally upregulated in Crohn's disease, it is only efficiently processed to CST during disease remission. Previous studies revealed higher plasma CgA levels during flare-ups as compared to ulcerative colitis and Crohn's disease patients in remission.³⁴ An open question remains how the levels of PST and CST are regulated in ulcerative colitis and Crohn's disease patients. For CST our findings suggest a proteolytic switch, where CgA and CST are excessively produced in Crohn's disease regardless of the disease state, but CgA is converted more into the anti-inflammatory CST in quiescent Crohn's disease. The gut barrier dysfunction in CST-KO mice is reminiscent of active Crohn's disease, because the gut permeability provided by cell-cell junctions is generally diminished in IBD patients.⁸⁴ Based on our findings, we hypothesize that the higher levels of CST during Crohn's disease remission promote anti-inflammatory responses and aid restoration of epithelial cellular junctions.

4 | MATERIAL AND METHODS

4.1 | Mice

Male wild type (WT), CST-knockout (KO) and CgA-KO mice (3 months old) on C57BL/6 background were kept in a 12 hours dark/light cycle on normal chow diet (NCD: 13.5% calorie from fat; LabDiet 5001, Lab Supply, Fort Worth, TX). Experiments were conducted in a blinded fashion whenever possible. For terminal procedure, mice were deeply anesthetized (assessed by pinching toe response) with isoflurane followed by harvesting of tissues. Euthanasia was achieved through exsanguination. For rescue experiments with exogenous CST and PST, mice were injected intraperitoneally with CST (2 µg/g body weight) and/or PST (2 µg/g body weight) at 9:00 AM for 2-4 weeks before collecting faeces or harvesting tissues. All mouse studies were approved by the UCSD and Veteran Affairs San Diego Institutional Animal Care and Use Committees and conform to relevant National Institutes of Health guidelines.

4.2 | Gut permeability assay

Fluorescein isothiocyanate conjugated dextran (FITC-dextran-FD4, 4 kDa; MilliporeSigma, St. Louis, MO) was administered (44 mg/100 g body weight) to 8 hours fasting mice by oral gavage followed by collection of blood after 4 hours of administration from the heart under deep isoflurane anaesthesia.⁸⁵ Plasma concentration of FITC was determined by comparison of fluorescence signals with a FITC-dextran standard curve.

4.3 | Measurement of tissue cytokines, CST, CgA and calprotectin

A portion of the colon was homogenized in PBS and cytokines were measured in 20 µL of the homogenate using U-PLEX mouse cytokine assay kit (Meso Scale Diagnostics, Rockville, MD) via the manufacturer's protocol. Mouse EIA kits from CUSABIO (CUSABIO Technology LLC, Houston, TX) were used to determine CgA (CSB-EL005344MO), CST (CSB-E17357m), and calprotectin (CSB-EQ013485MO).

4.4 | Determination of CgA and CST levels in human plasma

EDTA-plasma was collected from patients with Crohn's disease (N = 89) and ulcerative colitis (N = 101) (Table S1) and healthy controls (N = 50). Intestinal inflammation was

assessed by colonoscopy. A flare-up was defined as histological and endoscopic disease activity, whereas remission entailed absence of endoscopic inflammation and histological disease activity. EDTA-plasma from healthy controls (Table S2) was obtained from the Mini Donor Service at the University Medical Center Utrecht. Samples were thawed and diluted 50-times with extraction buffer (PBS with 0.5% Tween and 0.05% sodium azide), thoroughly vortexed followed by incubation at 4°C for 20 minutes on a rolling device. Afterwards samples were centrifuged at 760× *g* for 20 minutes at 4°C and the supernatant was collected for analysis. Samples were collected in compliance with the Declaration of Helsinki. EDTA plasma was used to quantify CgA and CST using ELISA (CUSABIO CSB-E17355h, CSB-E09153h). Informed consent was obtained, and the study was conducted in accordance with the Institutional Board Review of the University Medical Center Utrecht (approval number NL35053.041.11 & 11-050).

4.5 | Colon histological stains and immunohistochemistry

Mouse colon was isolated, washed in PBS and dehydrated in ethanol series, xylene and paraffin. Afterwards, the tissue was embedded in paraffin, formalin fixed, and paraffin embedded (FFPE) and sections of 5 µm were cut. Haematoxylin and eosin (HE) and Masson's trichrome (MT) staining were performed using standard techniques. For the immunohistochemistry, the tissue was heated in citrate buffer (pH 6.0, 1.0 nmol/L citric acid) and endogenous peroxidase activity was quenched with 3% H₂O₂ in methanol. Standard indirect immunoperoxidase procedures were used for detection (Vectastain and SK-4800, Vector Laboratories) with the antibody Rabbit-αKi-67 (1:100, Novus Biologicals), Rat-αF4/80 (1:500, Caltag laboratories and slides were counterstained with Mayer's haematoxylin. Followed by mounting using Quick D mounting medium. For fluorescent staining, slides were incubated with Rabbit-αCASPIII antibody (1:100, ab2302, Abcam) and nuclear counterstain with DAPI using Fluoromount-G (0100-01, Southern Biotech). Slides were imaged using the PerkinElmer Vectra (Vectra 3.0.3; PerkinElmer, MA) at 20x magnification or imaged using the Leica SP8 with a water dipping objective.

4.6 | Transmission Electron Microscopy (TEM) and morphometric analysis

To displace blood and wash tissues before fixation, mice were cannulated through the apex of the heart and perfused with a Ca²⁺ and Mg²⁺ free buffer composed of DPBS and 9.46 mmol/L KCl as described.⁷³ Mouse and human colon

fixation, embedding, sectioning and staining were done as described.⁷³ Grids were viewed using a JEOL JEM1400-plus TEM (JEOL, Peabody, MA) and photographed using a Gatan OneView digital camera with 4×4k resolution (Gatan, Pleasanton, CA). Morphometric analyses of the dense core vesicles were determined as described.⁸⁶ TJ length and diameter were determined by measuring the lengths and perpendicular widths using the line tool in NIH ImageJ software.

4.7 | Tight junction protein analysis via immunoblotting

Mouse colon pieces were homogenized in a buffer containing phosphatase and protease inhibitors, as previously described.¹⁹ Colon lysates were subjected to SDS-PAGE and immunoblotted. Followed by staining with Rabbit-αOccludin (1:1000, ab216327, Abcam, Cambridge, MA, USA), Rabbit-αClaudin 1 (1:2000, ab180158, Abcam), Rabbit-αClaudin 2 (2µg/ml, 51-6100, Thermo Fisher Scientific, Waltham, MA, USA), Mouse-αE-cadherin (1:500, 610182, BD Biosciences, San Jose, CA, USA), Rabbit-αcatenin (1:1000, C2081, Sigma-Aldrich, St. Louis, MO, USA) or Rat-αZO-1 (1:500, R26.4C, DSHB, Iowa City, Iowa, USA).

4.8 | Flow cytometry analysis

Isolated colon cells from digested mouse colon were stained with fluorescence-tagged antibodies to detect macrophages (CD45⁺CD11b⁺Emr1⁺) and helper T cells (CD45⁺CD4⁺). Data were analysed using FlowJo.

4.9 | Microbiome analysis

DNA was extracted from cecum of WT, CST-KO and CgA-KO (normal chow diet (NCD), littermates) using the Zymobiomics miniprep kit. Isolated DNA was quantified by Qubit (Thermo Fisher Scientific). DNA libraries were prepared using the Illumina Nextera XT library preparation kit. Library quantity and quality was assessed with Qubit and TapeStation (Agilent Technologies). Libraries were sequenced on Illumina HiSeq platform 2×150bp. Unassembled sequencing reads were directly analysed by CosmosID bioinformatics platform (CosmosID)⁸⁷ for multi-kingdom microbiome analysis and profiling of antibiotic resistance and virulence genes and quantification of organism's relative abundance. This system utilizes curated genome databases and a high-performance data-mining algorithm that rapidly disambiguates hundreds of millions of metagenomic sequence reads into the discrete microorganisms engendering the particular sequences. Data mining, interpretation and comparison of

taxonomic information from the metagenomic datasets were performed using Calyspo Bioinformatics software V.8.84.

4.10 | Real time PCR

Total RNA from colon tissue was isolated using RNeasy Mini Kit and reverse-transcribed using qScript cDNA synthesis kit. cDNA samples were amplified using PERFECTA SYBR FASTMIX L-ROX 1250 and analysed on an Applied Biosystems 7500 Fast Real-Time PCR system. Primer sequences are in Table S3. All PCRs were normalized to *Rplp0*, and relative expression levels were determined by the $\Delta\Delta C_t$ method as described.²⁴

4.11 | Statistics

Statistics were performed with PRISM 8 (version 8.4.3; San Diego, CA). Data were analysed using either unpaired two-tailed Student's *t* test for comparison of two groups or one-way or two-way analysis of variance for comparison of more than two groups followed by Tukey's *post hoc* test if appropriate. All data are presented as mean \pm SEM and significance were assumed when $P < .05$.

ACKNOWLEDGEMENTS

The authors thank Zbigniew Mikulski (La Jolla Institute for Immunology, CA, USA) and Kiek Verrijp (Radboud University Medical Center, Netherland) for technical support with the histology and immunohistochemistry. This work was supported by grants from the Veterans Affairs (I01 BX003934 to SKM), the Human Frontier Science Program (HFSP; RGY0080/2018 to G.v.d.B), the Netherlands Organization for Scientific Research (NWO-ALWVIDI864.14.001 to G.v.d.B), and European Research Council (grant agreement No. 862137 to G.v.d.B). GC is supported by grants from the Swedish Research Council and the Swedish Society for Medical Research. SEA is funded by is supported by a Rosalind Franklin Fellowship, co-funded by the European Union and University of Groningen, The Netherlands. EMM is supported by a Short-Term EMBO Fellowship (EMBO7887).

CONFLICTS OF INTEREST

The authors declare no conflict of interest.

DATA AVAILABILITY STATEMENT

Primary data available from the corresponding authors on reasonable request.

ORCID

Sushil K. Mahata  <https://orcid.org/0000-0002-8300-9873>

REFERENCES

1. Sender R, Fuchs S, Milo R. Revised estimates for the number of human and bacteria cells in the body. *PLoS Biol.* 2016;14(8):e1002533.
2. Wassenaar TM, Zimmermann K. Lipopolysaccharides in food, food supplements, and probiotics: should we be worried? *Eur J Microbiol Immunol (Bp).* 2018;8(3):63-69.
3. Perez-Reytor D, Jana V, Pavez L, Navarrete P, Garcia K. Accessory toxins of vibrio pathogens and their role in epithelial disruption during infection. *Front Microbiol.* 2018;9:2248.
4. Sartor RB, Wu GD. Roles for intestinal bacteria, viruses, and fungi in pathogenesis of inflammatory bowel diseases and therapeutic approaches. *Gastroenterology.* 2017;152(2):327-339.e324.
5. Weber CR, Raleigh DR, Su L, et al. Epithelial myosin light chain kinase activation induces mucosal interleukin-13 expression to alter tight junction ion selectivity. *J Biol Chem.* 2010;285(16):12037-12046.
6. Marchiando AM, Shen L, Graham WV, et al. Caveolin-1-dependent occludin endocytosis is required for TNF-induced tight junction regulation in vivo. *J Cell Biol.* 2010;189(1):111-126.
7. Scharl M, Paul G, Barrett KE, McCole DF. AMP-activated protein kinase mediates the interferon-gamma-induced decrease in intestinal epithelial barrier function. *J Biol Chem.* 2009;284(41):27952-27963.
8. Ye D, Ma I, Ma TY. Molecular mechanism of tumor necrosis factor-alpha modulation of intestinal epithelial tight junction barrier. *Am J Physiol Gastrointest Liver Physiol.* 2006;290(3):G496-G504.
9. Meyer-Hoffert U, Hornef MW, Henriques-Normark B, et al. Secreted enteric antimicrobial activity localises to the mucus surface layer. *Gut.* 2008;57(6):764-771.
10. Chakaroun RM, Massier L, Kovacs P. Gut microbiome, intestinal permeability, and tissue bacteria in metabolic disease: perpetrators or bystanders? *Nutrients.* 2020;12(4):1082.
11. Buckley A, Turner JR. Cell biology of tight junction barrier regulation and mucosal disease. *Cold Spring Harb Perspect Biol.* 2018;10(1):a029314.
12. Lutter L, Hoytema van Konijnenburg DP, Brand EC, Oldenburg B, van Wijk F. The elusive case of human intraepithelial T cells in gut homeostasis and inflammation. *Nat Rev Gastroenterol Hepatol.* 2018;15(10):637-649.
13. Winkler H, Fischer-Colbrie R. The chromogranins A and B: the first 25 years and future perspectives. *Neuroscience.* 1992;49(3):497-528.
14. El-Salhy M, Patcharatrakul T, Hatlebakk JG, Hausken T, Gilja OH, Gonlachanvit S. Chromogranin A cell density in the large intestine of Asian and European patients with irritable bowel syndrome. *Scand J Gastroenterol.* 2017;52(6-7):691-697.
15. Videen JS, Mezger MS, Chang YM, O'Connor DT. Calcium and catecholamine interactions with adrenal chromogranins. Comparison of driving forces in binding and aggregation. *J Biol Chem.* 1992;267(5):3066-3073.
16. Taupenot L, Harper KL, Mahapatra NR, Parmer RJ, Mahata SK, O'Connor DT. Identification of a novel sorting determinant for the regulated pathway in the secretory protein chromogranin A. *J Cell Sci.* 2002;115(Pt 24):4827-4841.
17. Borges R, Diaz-Vera J, Dominguez N, Arnau MR, Machado JD. Chromogranins as regulators of exocytosis. *J Neurochem.* 2010;114(2):335-343.

18. Gayen JR, Saberi M, Schenk S, et al. A novel pathway of insulin sensitivity in chromogranin a null mice: a crucial role for pancreastatin in glucose homeostasis. *J Biol Chem*. 2009;284:28498-28509.
19. Bandyopadhyay GK, Vu CU, Gentile S, et al. Catestatin (chromogranin A(352–372)) and novel effects on mobilization of fat from adipose tissue through regulation of adrenergic and leptin signaling. *J Biol Chem*. 2012;287(27):23141-23151.
20. Bandyopadhyay GK, Lu M, Avolio E, et al. Pancreastatin-independent inflammatory signaling mediates obesity-induced insulin resistance. *Diabetes*. 2015;64(1):104-116.
21. Bandyopadhyay GK, Mahata SK. Chromogranin A regulation of obesity and peripheral insulin sensitivity. *Front Endocrinol (Lausanne)*. 2017;8:20.
22. Mahapatra NR, O'Connor DT, Vaingankar SM, et al. Hypertension from targeted ablation of chromogranin A can be rescued by the human ortholog. *J Clin Invest*. 2005;115(7):1942-1952.
23. Biswas N, Gayen J, Mahata M, Su Y, Mahata SK, O'Connor DT. Novel peptide isomer strategy for stable inhibition of catecholamine release: application to hypertension. *Hypertension*. 2012;60(6):1552-1559.
24. Mahata SK, Kiranmayi M, Mahapatra NR. Catestatin: a master regulator of cardiovascular functions. *Curr Med Chem*. 2018;25(11):1352-1374.
25. Mahata SK, Corti A. Chromogranin A and its fragments in cardiovascular, immunometabolic, and cancer regulation. *Ann NY Acad Sci*. 2019;1455(1):34-58.
26. Rabbi MF, Labis B, Metz-Boutigue MH, Bernstein CN, Ghia JE. Catestatin decreases macrophage function in two mouse models of experimental colitis. *Biochem Pharmacol*. 2014;89(3):386-398.
27. Ying W, Mahata S, Bandyopadhyay GK, et al. Catestatin inhibits obesity-induced macrophage infiltration and inflammation in the liver and suppresses hepatic glucose production. Leading to improved insulin sensitivity. *Diabetes*. 2018;67(5):841-848.
28. Eissa N, Hussein H, Hendy GN, Bernstein CN, Ghia JE. Chromogranin-A and its derived peptides and their pharmacological effects during intestinal inflammation. *Biochem Pharmacol*. 2018;152:315-326.
29. Kojima M, Ozawa N, Mori Y, et al. Catestatin prevents macrophage-driven atherosclerosis but not arterial injury-induced neointimal hyperplasia. *Thromb Haemost*. 2018;118(1):182-194.
30. Muntjewerff EM, Dunkel G, Nicolassen MJT, Mahata SK, van den Bogaart G. Catestatin as a target for treatment of inflammatory diseases. *Front Immunol*. 2018;9:2199.
31. Mahata SK, O'Connor DT, Mahata M, et al. Novel autocrine feedback control of catecholamine release. A discrete chromogranin a fragment is a noncompetitive nicotinic cholinergic antagonist. *J Clin Invest*. 1997;100(6):1623-1633.
32. Mahata SK, Mahata M, Fung MM, O'Connor DT. Catestatin: a multifunctional peptide from chromogranin A. *Regul Pept*. 2010;162(1-3):33-43.
33. Tatemoto K, Efendic S, Mutt V, Makk G, Feistner GJ, Barchas JD. Pancreastatin, a novel pancreatic peptide that inhibits insulin secretion. *Nature*. 1986;324(6096):476-478.
34. Zissimopoulos A, Vradelis S, Konialis M, et al. Chromogranin A as a biomarker of disease activity and biologic therapy in inflammatory bowel disease: a prospective observational study. *Scand J Gastroenterol*. 2014;49(8):942-949.
35. Sciola V, Massironi S, Conte D, et al. Plasma chromogranin a in patients with inflammatory bowel disease. *Inflamm Bowel Dis*. 2009;15(6):867-871.
36. Wagner M, Stridsberg M, Peterson CG, Sangfelt P, Lampinen M, Carlson M. Increased fecal levels of chromogranin A, chromogranin B, and secretoneurin in collagenous colitis. *Inflammation*. 2013;36(4):855-861.
37. Zivkovic PM, Matetic A, Tadin Hadjina I, et al. Serum catestatin levels and arterial stiffness parameters are increased in patients with inflammatory bowel disease. *J Clin Med*. 2020;9(3):628.
38. Ying W, Tang K, Avolio E, et al. Immunosuppression of macrophages underlies the cardioprotective effects of CST (Catestatin). *Hypertension*. 2021;77 (5):1670–1682. <http://dx.doi.org/10.1161/hypertensionaha.120.16809>
39. Jiang Q, Taupenot L, Mahata SK, et al. Proteolytic cleavage of chromogranin A (CgA) by plasmin: selective liberation of a specific bioactive CgA fragment that regulates catecholamine release. *J Biol Chem*. 2001;276:25022-25029.
40. Biswas N, Rodriguez-Flores JL, Courel M, et al. Cathepsin L colocalizes with chromogranin a in chromaffin vesicles to generate active peptides. *Endocrinology*. 2009;150(8):3547-3557.
41. O'Connor DT, Kailasam MT, Kennedy BP, Ziegler MG, Yanaihara N, Parmer RJ. Early decline in the catecholamine release-inhibitory peptide catestatin in humans at genetic risk of hypertension. *J Hypertens*. 2002;20:1335-1345.
42. Chen Y, Wang X, Yang C, et al. Decreased circulating catestatin levels are associated with coronary artery disease: the emerging anti-inflammatory role. *Atherosclerosis*. 2019;281:78-88.
43. Ottesen A, Carlson CR, Louch WE, et al. Glycosylated chromogranin A in heart failure. *Circ Heart Fail*. 2017;10(2):e003675. <http://dx.doi.org/10.1161/circheartfailure.116.003675>
44. Ma TY, Iwamoto GK, Hoa NT, et al. TNF-alpha-induced increase in intestinal epithelial tight junction permeability requires NF-kappa B activation. *Am J Physiol Gastrointest Liver Physiol*. 2004;286(3):G367-G376.
45. Gross A, Pack LAP, Schacht GM, et al. Desmoglein 2, but not desmocollin 2, protects intestinal epithelia from injury. *Mucosal Immunol*. 2018;11(6):1630-1639.
46. Heiskala M, Peterson PA, Yang Y. The roles of claudin superfamily proteins in paracellular transport. *Traffic*. 2001;2(2):93-98.
47. Adams RB, Planchon SM, Roche JK. IFN-gamma modulation of epithelial barrier function. Time course, reversibility, and site of cytokine binding. *J Immunol*. 1993;150(6):2356-2363.
48. Howe KL, Reardon C, Wang A, Nazli A, McKay DM. Transforming growth factor-beta regulation of epithelial tight junction proteins enhances barrier function and blocks enterohemorrhagic Escherichia coli O157:H7-induced increased permeability. *Am J Pathol*. 2005;167(6):1587-1597.
49. Zhernakova A, Kurilshikov A, Bonder MJ, et al. Population-based metagenomics analysis reveals markers for gut microbiome composition and diversity. *Science*. 2016;352(6285):565-569.
50. Costa F, Mumolo MG, Ceccarelli L, et al. Calprotectin is a stronger predictive marker of relapse in ulcerative colitis than in Crohn's disease. *Gut*. 2005;54(3):364-368.
51. Eichner M, Protze J, Piontek A, Krause G, Piontek J. Targeting and alteration of tight junctions by bacteria and their virulence factors such as Clostridium perfringens enterotoxin. *Pflugers Arch*. 2017;469(1):77-90.

52. Rabbi MF, Munyaka PM, Eissa N, Metz-Boutigue MH, Khafipour E, Ghia JE. Human catestatin alters gut microbiota composition in mice. *Front Microbiol.* 2016;7:2151.
53. Michielan A, D'Inca R. Host-microbiome interaction in Crohn's disease: a familiar or familial issue? *World J Gastrointest Pathophysiol.* 2015;6(4):159-168.
54. Packey CD, Sartor RB. Commensal bacteria, traditional and opportunistic pathogens, dysbiosis and bacterial killing in inflammatory bowel diseases. *Curr Opin Infect Dis.* 2009;22(3):292-301.
55. Rabbi MF, Eissa N, Munyaka PM, et al. Reactivation of intestinal inflammation is suppressed by catestatin in a murine model of colitis via M1 macrophages and not the gut microbiota. *Front Immunol.* 2017;8:985.
56. Lee JC, Taylor CV, Gaucher SP, et al. Primary sequence characterization of catestatin intermediates and peptides defines proteolytic cleavage sites utilized for converting chromogranin A into active catestatin secreted from neuroendocrine chromaffin cells. *Biochemistry.* 2003;42(23):6938-6946.
57. Benyamin B, Maihofer AX, Schork AJ, et al. Identification of novel loci affecting circulating chromogranins and related peptides. *Hum Mol Genet.* 2017;26(1):233-242.
58. Dasgupta A, Bandyopadhyay GK, Ray I, et al. Catestatin improves insulin sensitivity by attenuating endoplasmic reticulum stress: In vivo and in silico validation. *Comput Struct Biotechnol J.* 2020;18:464-481.
59. Eissa N, Elgazzar O, Hussein H, Hendy GN, Bernstein CN, Ghia JE. Pancreastatin reduces alternatively activated macrophages, disrupts the epithelial homeostasis and aggravates colonic inflammation. A descriptive analysis. *Biomedicines.* 2021;9(2):134.
60. Al-Sadi R, Ye D, Dokladny K, Ma TY. Mechanism of IL-1beta-induced increase in intestinal epithelial tight junction permeability. *J Immunol.* 2008;180(8):5653-5661.
61. Su L, Nalle SC, Shen L, et al. TNFR2 activates MLCK-dependent tight junction dysregulation to cause apoptosis-mediated barrier loss and experimental colitis. *Gastroenterology.* 2013;145(2):407-415.
62. Mankertz J, Amasheh M, Krug SM, et al. TNFalpha up-regulates claudin-2 expression in epithelial HT-29/B6 cells via phosphatidylinositol-3-kinase signaling. *Cell Tissue Res.* 2009;336(1):67-77.
63. Suzuki T, Yoshinaga N, Tanabe S. Interleukin-6 (IL-6) regulates claudin-2 expression and tight junction permeability in intestinal epithelium. *J Biol Chem.* 2011;286(36):31263-31271.
64. van der Post S, Jabbar KS, Birchenough G, et al. Structural weakening of the colonic mucus barrier is an early event in ulcerative colitis pathogenesis. *Gut.* 2019;68(12):2142-2151.
65. Schlegel N, Boerner K, Waschke J. Targeting desmosomal adhesion and signalling for intestinal barrier stabilization in inflammatory bowel diseases-Lessons from experimental models and patients. *Acta Physiol (Oxf).* 2021;231(1):e13492.
66. Saia RS, Ribeiro AB, Giusti H. Cholecystokinin modulates the mucosal inflammatory response and prevents the lipopolysaccharide-induced intestinal epithelial barrier dysfunction. *Shock.* 2020;53(2):242-251.
67. Wu R, Dong W, Cui X, et al. Ghrelin down-regulates proinflammatory cytokines in sepsis through activation of the vagus nerve. *Ann Surg.* 2007;245(3):480-486.
68. Drucker DJ, Habener JF, Holst JJ. Discovery, characterization, and clinical development of the glucagon-like peptides. *J Clin Invest.* 2017;127(12):4217-4227.
69. Ottaway CA, Lewis DL, Asa SL. Vasoactive intestinal peptide-containing nerves in Peyer's patches. *Brain Behav Immun.* 1987;1(2):148-158.
70. Keita AV, Carlsson AH, Cigehn M, Ericson AC, McKay DM, Soderholm JD. Vasoactive intestinal polypeptide regulates barrier function via mast cells in human intestinal follicle-associated epithelium and during stress in rats. *Neurogastroenterol Motil.* 2013;25(6):e406-e417.
71. Izu LT, McCulle SL, Ferreri-Jacobia MT, Devor DC, Duffey ME. Vasoactive intestinal peptide-stimulated Cl⁻ secretion: activation of cAMP-dependent K⁺ channels. *J Membr Biol.* 2002;186(3):145-157.
72. Conlin VS, Wu X, Nguyen C, et al. Vasoactive intestinal peptide ameliorates intestinal barrier disruption associated with Citrobacter rodentium-induced colitis. *Am J Physiol Gastrointest Liver Physiol.* 2009;297(4):G735-G750.
73. Dethlefsen L, McFall-Ngai M, Relman DA. An ecological and evolutionary perspective on human-microbe mutualism and disease. *Nature.* 2007;449(7164):811-818.
74. Lemichez E, Lecuit M, Nassif X, Bourdoulous S. Breaking the wall: targeting of the endothelium by pathogenic bacteria. *Nat Rev Microbiol.* 2010;8(2):93-104.
75. Chin AC, Flynn AN, Fedwick JP, Buret AG. The role of caspase-3 in lipopolysaccharide-mediated disruption of intestinal epithelial tight junctions. *Can J Physiol Pharmacol.* 2006;84(10):1043-1050.
76. Cani PD, Amar J, Iglesias MA, et al. Metabolic endotoxemia initiates obesity and insulin resistance. *Diabetes.* 2007;56(7):1761-1772.
77. Dao MC, Everard A, Aron-Wisniewsky J, et al. Akkermansia muciniphila and improved metabolic health during a dietary intervention in obesity: relationship with gut microbiome richness and ecology. *Gut.* 2016;65(3):426-436.
78. Everard A, Belzer C, Geurts L, et al. Cross-talk between Akkermansia muciniphila and intestinal epithelium controls diet-induced obesity. *Proc Natl Acad Sci USA.* 2013;110(22):9066-9071.
79. Moreira AP, Texeira TF, Ferreira AB, Peluzio Mdo C, Alfnas RC. Influence of a high-fat diet on gut microbiota, intestinal permeability and metabolic endotoxaemia. *Br J Nutr.* 2012;108(5):801-809.
80. Johne B, Fagerhol MK, Lyberg T, et al. Functional and clinical aspects of the myelomonocyte protein calprotectin. *Mol Pathol.* 1997;50(3):113-123.
81. Mulak A, Koszewicz M, Panek-Jeziorna M, Kozirowska-Gawron E, Budrewicz S. Fecal calprotectin as a marker of the gut immune system activation is elevated in Parkinson's disease. *Front Neurosci.* 2019;13:992.
82. von Martels JZH, Bourgonje AR, Harmsen HJM, Faber KN, Dijkstra G. Assessing intestinal permeability in Crohn's disease patients using orally administered 52Cr-EDTA. *PLoS One.* 2019;14(2):e0211973.
83. Berstad A, Arslan G, Folvik G. Relationship between intestinal permeability and calprotectin concentration in gut lavage fluid. *Scand J Gastroenterol.* 2000;35(1):64-69.
84. Turpin W, Lee S-H, Raygoza Garay JA, et al. Increased intestinal permeability is associated with later development of Crohn's disease. *Gastroenterology.* 2020;159(6):2092-2100.e5. <http://dx.doi.org/10.1053/j.gastro.2020.08.005>
85. Woting A, Blaut M. Small intestinal permeability and gut-transit time determined with low and high molecular weight fluorescein isothiocyanate-dextrans in C3H mice. *Nutrients.* 2018;10(6):685.
86. Pasqua T, Mahata S, Bandyopadhyay GK, et al. Impact of Chromogranin A deficiency on catecholamine storage,

catecholamine granule morphology and chromaffin cell energy metabolism in vivo. *Cell Tissue Res.* 2016;363(3):693-712.

87. Lax S, Smith DP, Hampton-Marcell J, et al. Longitudinal analysis of microbial interaction between humans and the indoor environment. *Science.* 2014;345(6200):1048-1052.

SUPPORTING INFORMATION

Additional Supporting Information may be found online in the Supporting Information section.

How to cite this article: Muntjewerff EM, Tang K, Lutter L, et al. Chromogranin A regulates gut permeability *via* the antagonistic actions of its proteolytic peptides. *Acta Physiol.* 2021;232:e13655. <https://doi.org/10.1111/apha.13655>